https://dx.doi.org/10.1016/j.conbuildmat.2015.12.164

Photocatalytic Pavements with Epoxy-Bonded TiO_2-Containing Spreading Material

D. Wang[a], Z. Leng[b1], M. Hüben[c], M. Oeser[a], B. Steinauer[a]

[a]Institut of Highway Engineering Aachen, RWTH Aachen, Germany

[b]Department of Civil and Environmental Engineering, Hong Kong Polytechnic University, Hong Kong SAR, China

[c]Fraunhofer-Institute for Molecular Biology and Applied Ecology, Germany

Abstract: Titanium dioxide (TiO_2) is a photocatalyst which can accelerate the oxidation of nitrogen oxides (NO_X) and other pollutants under ultraviolet (UV) radiation. In this study, a new method to coat TiO_2 onto asphalt pavements was developed with the aim to enhance the NO_X decomposition efficiency and durability of the coating material for asphalt pavements. In this method, pulverized TiO_2-cement mortar is used as the spreading material, which is bonded to asphalt pavement surface by epoxy resin. The composition of the TiO_2-cement mortar was optimized in terms of its mechanical properties. The long-term NO_X degradation efficiency, abrasion resistance, and skid resistance of the spreading material were measured after it was subjected to 300 min polishing by the advanced Aachen Polishing Machine (APM). It was concluded that durable NO_X degradation efficiency can be achieved by the developed method and the method is feasible for practical implementation.

[1]Corresponding Author: Zhen Leng, PhD, Assistant Professor, Department of Civil and Environmental Engineering, The Hong Kong Polytechnic University, Email: zhen.leng@polyu.edu.hk, PN: (+852)27666007

Keywords: Photocatalytic pavements, Asphalt pavements, Epoxy-bonded spreading material, NO removal efficiency, Polishing resistance

1. Introduction

Functional pavements, which provide not only smooth riding surfaces to vehicles, but also various additional functions, such as mitigating traffic noise, decreasing road surface temperature, and degrading harmful vehicle gases, have been extensively studied recently [1-3]. Among these emerging pavements, photocatalytic pavements have gained rapidly increasing interest, because of their function of purifying vehicle emissions.

Within vehicle emissions, nitrogen oxides (NO_X) is one of the main hazardous substances. It is also the major precursor of particulate matter 2.5 (PM 2.5), the representative air pollutant of photo-chemical smog and haze [4]. Although various types of gas-cleaning equipment have been developed and installed to vehicles, the NO_X concentration within road vicinity is still quite high, especially in urban areas with high traffic densities. To further improve the air quality of road environment, attempts have been made to build photocatalytic pavements which have the function of degrading NO_X. So far, the most common and effective technology is to apply titanium dioxide (TiO_2) particles onto road surface, since TiO_2 is capable of accelerating the photocatalytic activity of NO_X under ultraviolet (UV) radiation, and it also has the advantages of high chemical stability, super-hydrophilicity, and relatively low cost. The feasibility of this technology in decreasing NO_X concentration has been verified by various studies [5-10].

To incorporate TiO_2 particles onto road surface, the simplest way is to apply a thin TiO_2 coating layer. Previous studies have shown that TiO_2 coating layers usually worked well on concrete pavements, but it remains a challenging task to coat TiO_2 onto asphalt pavements [11-14], which are the dominant type of pavements in the world. The major problems of applying TiO_2 to asphalt pavements include relatively low photocatalytic efficiency and poor durability under traffic effect. Thus, technologies that can further enhance the NO_X degradation efficiency and durability of the TiO_2 coating for asphalt pavements are keenly desired.

In this study, to build functional asphalt pavements with durable NO_X degradation efficiency, a new method has been developed, which bonds pulverized TiO_2-cement mortar to asphalt pavement surface by epoxy resin. To investigate and optimize the performance of this new method, the following tasks were conducted:

1. Select the appropriate TiO_2 product;
2. Optimize the composition of TiO_2-containing spreading material in terms of its mechanical properties through laboratory testing;
3. Apply the optimized spreading material to a test asphalt pavement section to evaluate its field application feasibility; and
4. Assess the long-term NOx degradation efficiency and skid resistance of the cores extracted from the test pavement.

2. Research background

2.1 Photocatalytic oxidation of NOx

The photocatalytic oxidation property of TiO_2 was discovered by Fujishima in 1972 [15]. With this property, TiO_2 can oxidize both organic pollutants and oxides such as nitric oxide (NO), nitrogendioxide (NO_2), and sulfurmonoxide (SO) under UV irradiation [16].

The photocatalytic oxidation begins with the irradiation of light over TiO_2 particles. When TiO_2 absorbs a photon containing the energy larger than or equal to its band gap, 3.2eV, an electron will be promoted from the valence band to the conduction band, leaving a hole behind and creating electron-hole pairs, which are also known as excitons [16, 17]. This process can be described by Eq. 1.

$$TiO_2 \xrightarrow{hv} h^+ + e^- \qquad (1)$$

In the above reaction, h^+ and e^- are powerful oxidizing and reducing agents, respectively. The strong oxidation power of h^+ enables it to react with water to generate the highly active hydroxyl radical ($OH^{\cdot}$), which is also a powerful oxidant. In addition, the power of the electrons can induce the reduction of molecular oxygen (O_2) to superoxide anion (O_2^-), which also has the strong capacity of degrading pollutants [17]. These two processes can be illustrated by Eq. 2 and 3, respectively.

$$h^+ + OH^- \rightarrow OH^* \qquad (2)$$

$$e^- + O_2 \rightarrow O_2^- \qquad (3)$$

The superoxide anion can further react with H^+ dissociated from water to generate the HO_2^* radical, as Eq. 4 shows.

$$H^+ + O_2^- \rightarrow HO_2^* \qquad (4)$$

Most organic air pollutants can be degraded completely by either the OH^- or the holes themselves to innocuous final products. For example, NO can be oxidized to NO_2, and then both the hazardous gases (NO and NO_2) can be degraded to water soluble nitrates, as Eq.5 and 6 show [15-19]:

$$NO + HO_2^* \rightarrow NO_2 + OH^* \quad (5)$$

$$NO_2 + OH^* \rightarrow HNO_3 \quad (6)$$

After the above reactions, the final product, nitric acid (HNO_3), can be easily washed away by rainwater.

2.2 Surface treatment of asphalt pavement with epoxy-bonded spreading material

To restore or improve the surface characteristics of pavements, it is a common practice in Germany and some other countries to treat pavement surface with epoxy-bonded spreading material, such as hard aggregate [20]. As illustrated in Figure 1, this treatment method involves first applying epoxy resin onto asphalt pavement surface and then compressing aggregate or other spreading material into epoxy. When the spreading material and epoxy are appropriately designed, this treatment method may provide the following beneficial functions:

- improving pavement skid resistance;
- reducing traffic noise; and
- decreasing temperature of asphalt pavements in hot days, therefore reducing their rutting potential.

Moreover, since the surface treatment can be completed within a few hours, early traffic opening is possible.

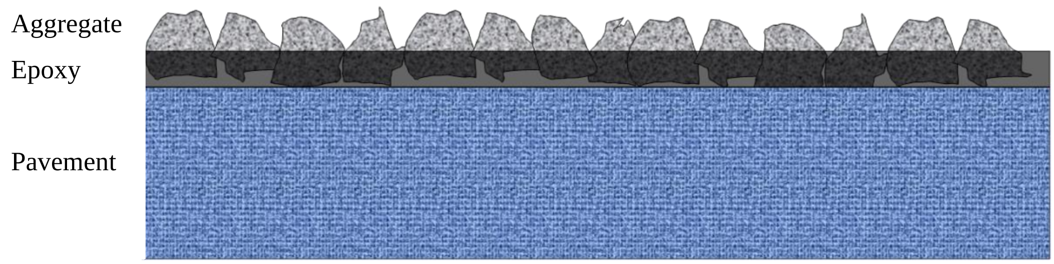

Figure 1: Surface treatment of asphalt pavement with epoxy-bonded spreading material

In this study, specially designed cement mortar containing TiO_2 were pulverized and used as the surface-treating spreading material to produce asphalt pavement with the function of air purification. Although this may slightly increase the initial construction cost of the spreading material, it brings additional air-purifying function to asphalt pavements. Moreover, this method has the following advantages compared to most other coating methods to produce photocatalytic asphalt pavements:

- There is no direct contact between TiO_2 and bitumen, which protects bitumen from the photocatalytic processes.
- Even with material loss due to polishing processes, TiO_2-containing surfaces would arise again and again, ensuring a long-lasting photocatalytic function.

3. Testing methods and equipment

The main property of the spreading material that was characterized in this study is the NO_x degradation efficiency. Since the spreading material is directly in contact with the vehicle tire, it is important that it can retain satisfying photocatalytic NO_x degradation efficiency under vehicle polishing. Thus, the advanced Aachen Polishing Machine (APM) was utilized in this study to apply simulated long-term tire polishing to the spreading material coated on asphalt pavements, and the NOx degradation efficiencies of the spreading materials both before and after polishing were measured to assess the durability of photocatalytic function of the spreading material. In addition, the surface characteristics, such as skid resistance and drainability, were also measured to ensure they can serve as a safe driving surface.

3.1 Measurement of NOx degradation efficiency

As Figure 2 shows, a test apparatus of the Fraunhofer Institute for Molecular Biology and Applied Ecology (IME) manufactured in accordance with ISO 22197-1 was used in this study to measure the NOx degradation efficiency of the testing samples with the standard dimensions of 10 cm × 5 cm × 1 cm [21].

Before each test was started, the testing sample was first cleaned with a brush and water. Then, the sample was irradiated at an intensity of 700 W/m^2 for 1 hour and slowly shaken for 1 hour in UHQ water. After drying for 1 hour at 60°C, the sample was stored in a dehydrator until the measurement was taken. Both the microscopic and macroscopic surface attachments were removed through this pre-treatment and the surface was to be transferred to a defined initial state.

A moisturized mixture of synthetic air and NO was then injected into the measurement cell holding the testing sample. The amount of NO was regulated so that a constant rate of 1 ppm was in the gas mixture. The volume flow was adjusted to 1 L/min and continuously controlled by a Fisher+Porter precision measuring tube. The relative humidity of the gas mixture was controlled between 50 and 60%.

(a) (b)

Figure 2: Measurement of NOx degradation efficiency: (a) Sunset radiation apparatus and Horibo NO_x analyzer; (b) test specimen (10 cm × 5 cm × 1 cm)

The measurement cell was irradiated and the NO content in the outflow gas mixture was continuously monitored according to the principle of chemiluminescence. During the radiation, the temperature was controlled between 25 and 30°C. As Figure 3 shows, the radiant energy of the xenon-lamp was 304 W/m^2 within the wavelength range of 290 to 800 nm. Within the wavelength range of 300 to 400 nm, which is relevant to the photocatalysis, the radiant energy was 46 W/m^2, which is comparable to the radiation intensity of the sun at mid-latitudes.

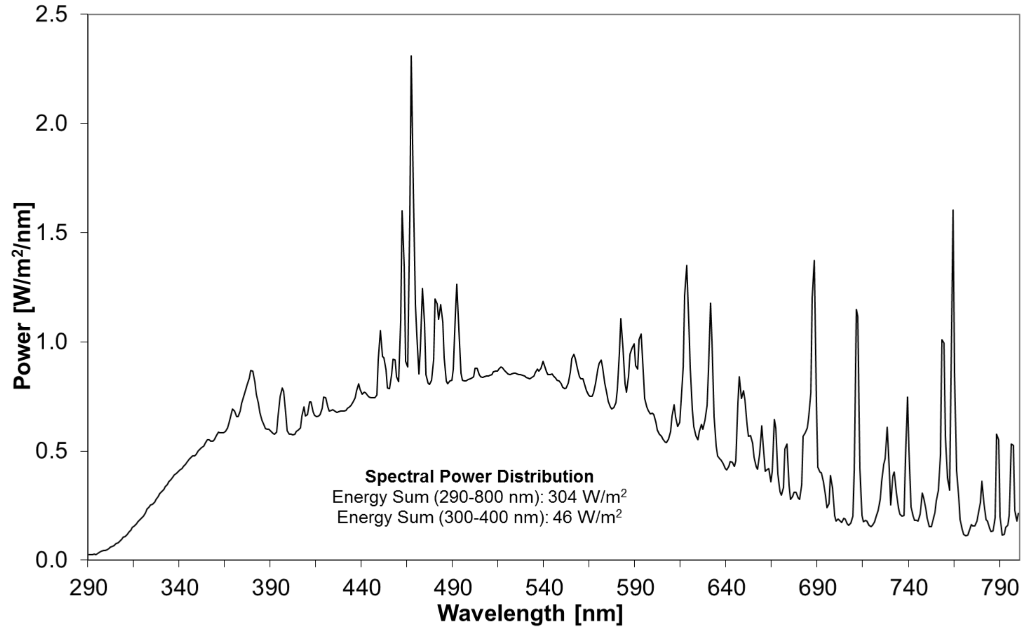

Figure 3: Spectral power distribution of the xenon-lamp light

3.2 Simulation of long-term tire polishing

The polishing resistance is critically important for pavement coating materials, because it directly affects the coating materials' durability. In this study, the polishing effect of tires was simulated by the advanced APM as shown in Figure 4 [22], which is equipped with real vehicle tires (Type: Vanco 8, 165/75 R 14 C 8PR 97/95 R TL from Continental).

The APM applies shear stresses to test plates by providing a superimposed translational and rotational motion. The translational motion is achieved by a horizontally movable sled onto which the test plates are fixed, while the rotational motion is realized by rotating two polishing wheels around the vertical axis. The polishing tires have an inner pressure of 0.2 MPa and an imposed load of 200 kg. The sled moves horizontally 9 times back and forth per minute, while the tires spin 41 rotations per minute. The horizontal distance between the centers of the two tires is 55 cm; the velocity of the circular motion is therefore about 1.2 m/s. Such configuration was designed to make the entire test plate subjected to equal polishing effect. Since dust on the road consists of about 60 to 80% SiO_2 by weight [22], quartz powder were selected as polishing agents. During a typical polishing test, polishing agent and water are spread evenly over the surface at a rate of 27±7 g/min. Based on the findings of the previous studies, the polishing duration was fixed at 300 min, because after 300 min of polishing, the test samples will reach equilibrium, and little or no changes will be caused by further polishing action [23, 24].

Figure 4: Aachen polishing machine

3.3 Measurement of surface characteristics of spreading material

To evaluate the effect of polishing on the surface characteristics of the spreading material, the following tests were conducted: 1) the pendulum test according to EN 13036-4 to measure the pendulum test value (PTV), which serves as an indicator of the skid resistance at low speed (approximately 10 km/h) (Figure 5a); 2) the Wehner/Schulze (W/S) test according to EN12697-49 to measure the dynamic skid resistance at 60 km/h according to EN 12697-49 (Figure 5b); and 3) the outflow test according to EN 13036-3 to measure the horizontal drainability (Figure 5c).

(a) (b) (c)

Figure 5: Tests to measure surface characteristics of spreading material: (a) pendulum test; (b) W/S test; (c) outflow test

4. Selection of TiO_2 material

To find the appropriate TiO_2 material to be mixed in the spreading material, a total of eight TiO_2 products (labelled as VU0 to VU7) were evaluated. Among these products, VU0 was the reference product, which was a commercial photocatalytically active cement mixture. The basic properties of the other seven products are shown in Table 1.

Table1 Basic properties of TiO_2 products

Variant	Modification	Grain Size [nm]	Surface Area (BET) [m^2/g]	pH	TiO_2 Content [M.-%]
1	anatase	15	> 225	4 to 9	87.5
2	anatase	15	> 225	3 to 11	85
3	rutile/anatase	120	10	5	65
4	rutile/anatase	150	10	4.5	59
5	anatase	150	10	7	100
6	anatase	15	90	2 to 3	90
7	anatase	15	90	1.5	99

With the selected eight TiO_2 products, standard samples were prepared in accordance with EN 196-1 [25], and their NO degradation efficiencies were measured using the apparatus described in Section 3.1. 4% of TiO_2 in terms of the weight of the cement was contained in each sample, including VU0, because previous studies have shown that when the TiO_2 content in cement is above 4%, the effect of increasing TiO_2 content on the photocatalytic efficiency is not significant any more [26], and 4% is also the standard TiO_2 content specified in EN196-1 to assess the photocatalytic efficiency of TiO_2 cement. The testing results are shown in Figure 6, and it can be observed that all samples were effective in decomposing NO but at very different levels (decomposition rates varying between 14% and 67%). The variation in NO decomposition rate is considered mainly due to the difference in the composition of the TiO_2 products. Previous studies have shown that anatase-type TiO_2 in general provides better photocatalytic efficiency compared to rutile-type TiO_2 [27]. Thus, the two products containing rutile, VU3 and VU4, provided the lowest NO decomposition rates. In addition, the TiO_2 content of the products also plays important role in the photocatalytic efficiency. Correspondingly, VU5, VU6 and VU7, which have higher TiO_2 contents, showed higher NO-decomposition rates, which are close to that of the reference product (VU0) or even slightly higher. Among VU5, VU6, and VU7, the performance of VU5 is worst, probably due to its smallest surface area. Based on these results, VU7 was finally selected for the following experimental study, since it provided the highest NO-decomposition rate.

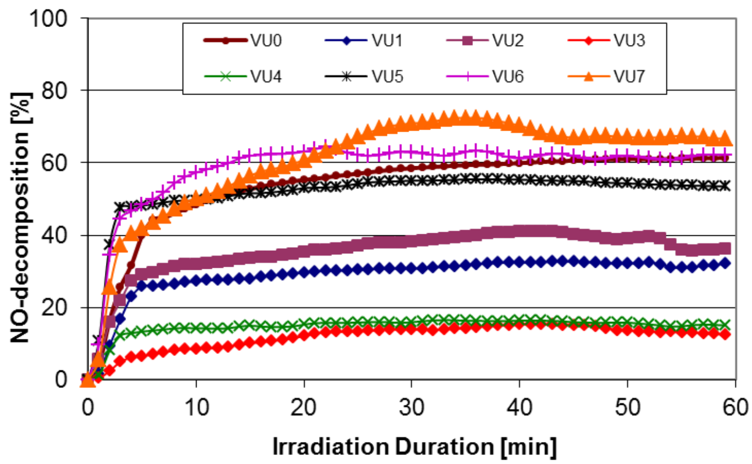

Figure 6: Mean NO degradation efficiencies for all specimens

Figure 7 presents the NO decomposition rates of VU7 when it is added to cement at different rates (4%, 7% and 10%) and under different UV irradiation levels (46 W/m^2 and 10 W/m^2 within the wavelength range from 300 to 400 nm). As aforementioned, 4% is the standard TiO_2 content for cement according to EN 196-1, while 10% is the maximum TiO_2 content according to the study by Bruse and Droll [26]. In addition, a TiO_2 content of 7% was added as a middle value between 4% and 10%. From Figure 7, it can be seen that the photocatalytic efficiency increases with the increase of TiO_2 content, and stronger irradiation energy results in faster NO decomposition.

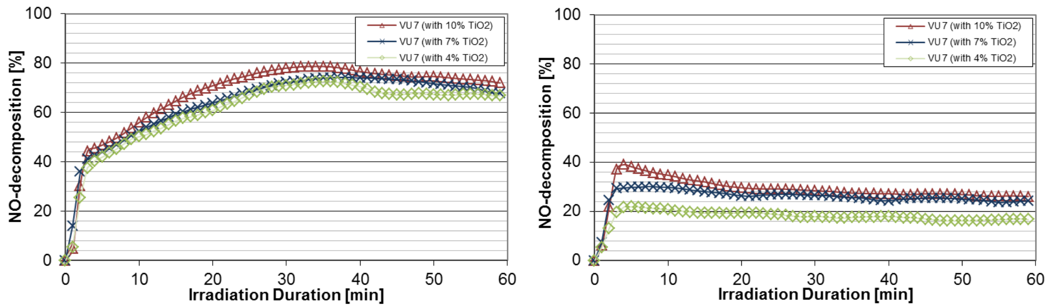

(a) (b)

Figure 7: Effect of the TiO_2 content on the photocatalytic activity with an irradiation energy of: (a) 46 W/m^2; (b) 10 W/m^2

5. Preparation and optimization of TiO_2-containing spreading material

In this study, the photocatalytic function of asphalt pavement was achieved by bonding TiO_2-containing spreading material, i.e., pulverized TiO_2-cement mortar, onto pavement surface with epoxy. Specimens with sufficient strength were first prepared by mixing cement, water, sand and TiO_2 (VU7). These specimens were then broken into small pieces after hardening and those with the sizes of 2 to 5 mm were collected through sieving. To maximize the polishing and wearing resistance, the preparation processes and the composition of the TiO_2-containing spreading material were optimized through systematic investigations.

To ensure the abrasion and skid resistance of the spreading material, testing specimens with different compositions were prepared. These specimens were first subjected to the polishing stresses from APM for 300 minutes, which is equivalent to the effect of 8 to 15 years of real traffic [28]. Then, their abrasion values were topographically measured with a texture meter and their skid resistances were determined by the pendulum test. As Figure 8 shows, the abrasion value is defined as the change in the mean height of the considered surface before and after polishing, which indicates the intensity of the material loss or abrasion.

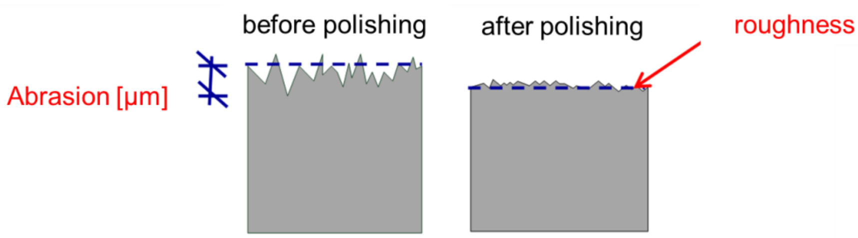

Figure 8: Schematic diagram of surface roughness change due to polishing

To investigate the effect of sand gradation, specimens with different fine and coarse sand ratios were prepared and tested. Figure 9 presents the results of the abrasion value and skid resistance tests for the mortar specimens with different 0.8/1.18mm and 0.2/0.4mm ratios. It can be seen that sand grain size has significant effect on the abrasion and long-term skid resistance development. Finer sand grains in the mortar (grain size: 0.2-0.4 mm) were better regarding skid resistance, while the trend for wearing resistance is opposite. With a ratio of 62% to 38% between coarser and finer grains, the optimum skid and wear resistance can be achieved. With this optimum grain size ratio, a PTV-value of 61 was measured, which clearly exceeds the minimum values specified in the regulation (51 for dense-graded asphalt pavement under the heaviest traffic volume and 54 for porous asphalt pavement under the heaviest traffic volume) [29]. In other words, these pulverized mortar grains can be used as spreading material on asphalt surfaces of all constructional designs.

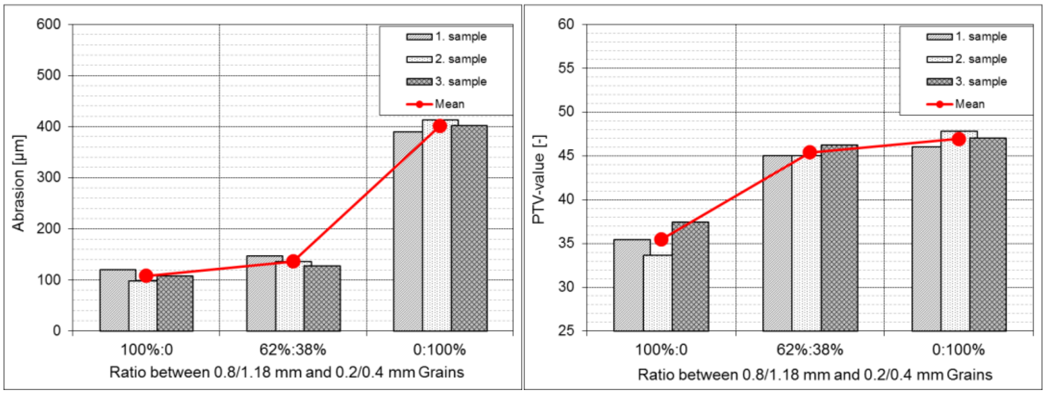

(a) (b)

Figure 9: Influence of grain size on: (a) wear resistance; (b) skid resistance

In addition to polishing and wearing resistance, the TiO_2-containing mortar grains must have sufficient strength to carry the dynamic traffic loads. Thus, compressive strength tests were conducted on TiO_2-containing mortar specimens with different compositions. As Figure 10 shows, the compressive strength of the specimens decreases with increasing water-cement ratio and sand-cement mixture ratio, but varying the TiO_2 content had insignificant effect on the compressive strength of the specimens.

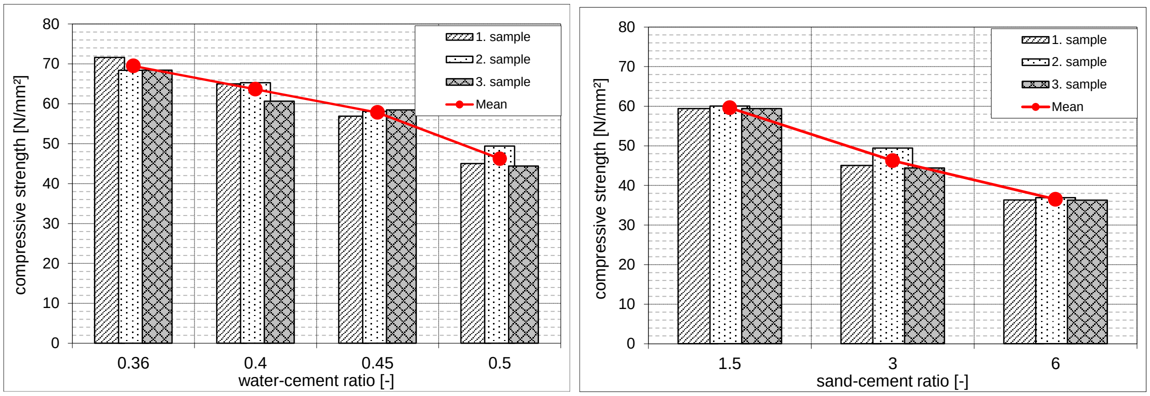

(a) (b)

Figure 10: Compressive strength vs: (a) water-cement ratio; (b) sand-cement ratio

Based on the polishing and wearing resistance test results, a sand-cement ratio of 1.5 and a water-cement ratio of 0.36 were selected to maximize the strength. Table 2 shows the percentages of the components of the finally selected mortar mixture.

Table 2 Components of TiO_2-cement mortar

Component		Mass Percentage (%)
Cement (CEM II 42.5 R)		33.6
TiO_2		1.4
Sand (D < 2 mm)	0.8/1.18mm (68%)	32.5
	0.2/0.4mm (32%)	19.9
Water		12.6

With the optimized mortar composition shown in Table 2, a compressive strength of 110 N/mm^2 was obtained. However, this value is still relatively low compared to those of natural rocks (120 to 220 N/mm^2). To further improve the strength of the spreading material, a mixture which consisted of pulverized TiO_2-cement mortar of the grain size of

2 to 4 mm and hard natural diabase of the grain size of 4 to 5 mm was produced (Figure 11). The diabase particles in relatively larger sizes were added to provide a stabilizing effect on the pulverized TiO_2-cement mortar, so that the tire stress applied to TiO_2-containing grains could be reduced. Obviously, the more diabase is added, the higher the resistance and the poorer the NO-elimination are expected. With a mass ratio of 1:1 between TiO_2-containing grains and diabase, it was found that an impact crushing value of 17% was achieved, which fulfils the requirement (maximum 18%) according to EN 1097-2 [30].

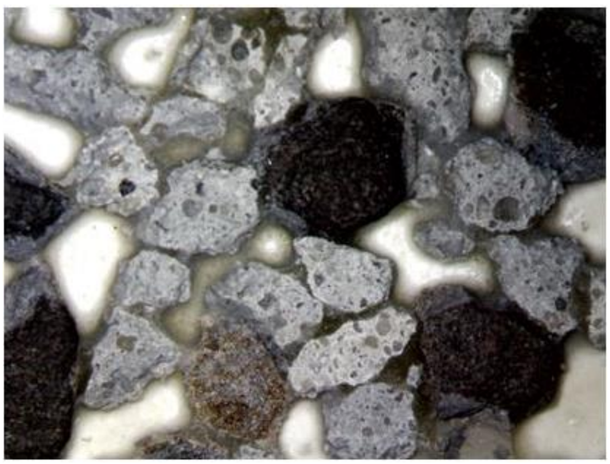

Figure 11: Mixture of TiO_2-containing grains in the grain size 2/4 mm (lighter grains) and impact-resistant diabase in the grain size 4/5 mm (darker grains)

6. Photocatalytic and mechanical durability of spreading materials under practical conditions

To further evaluate the photocatalytic and mechanical durability of the TiO_2-containing spreading materials under practical conditions, a test section was built at the Institute of

Highway Engineering at Aachen, Germany. The asphalt mixture paving of this test section was carried out using a small paver and a roller compactor, as shown in Figure 12. Care was taken during construction so that the applied asphalt mixture could have practice-oriented output properties. Then, the asphalt pavement surface was coated with epoxy resin, on top of which the TiO_2-containing spreading material 2 to 5mm in size was applied. The amount of epoxy was selected so that the spreading material particles are embedded to about half of their diameter. Finally, the excessive spreading material was swept away using a broom after the hardening of the epoxy. The pictures in Figure 13 illustrate the process of applying TiO_2-containing spreading material.

(a) (b) (c)

Figure 12: Asphalt mixture paving of test section: (a) test section before asphalt paving; (b) paving of asphalt mixture; (c) compaction of asphalt mixture

(a) (b) (c)

Figure 13: Application of the epoxy and spreading material: (a) applying epoxy resin; (b)

applying spreading materials and removing the excessive ones; (c) final asphalt pavement surface treated with spreading material

After the epoxy applied to the asphalt pavement is completely cured, cores with a diameter of 225 mm were extracted from the test section. These cores were then embedded into concrete plates, as shown in Figure 14, and subjected to polishing stress by APM for 300 mins.

Figure 14: Drilled core from the test track after 300 mins polishing

Figure 15 plots the NO-decomposition test results of the cores before and after polishing. It can be seen that in the unpolished state, a NO-decomposition rate of 25.2 % was achieved. After 300 mins of APM polishing (equivalent to the polishing effect of 8 to 15 year traffic), the NO-decomposition rate was reduced. However, it was still at a level of around 10.7%. This indicates that the spreading material could effectively degrade NOx during its lifetime. It is worth noting that in this study, 4% of TiO_2 was added to cement. If a higher TiO_2 content is used, a higher NO-decomposition rate is expected.

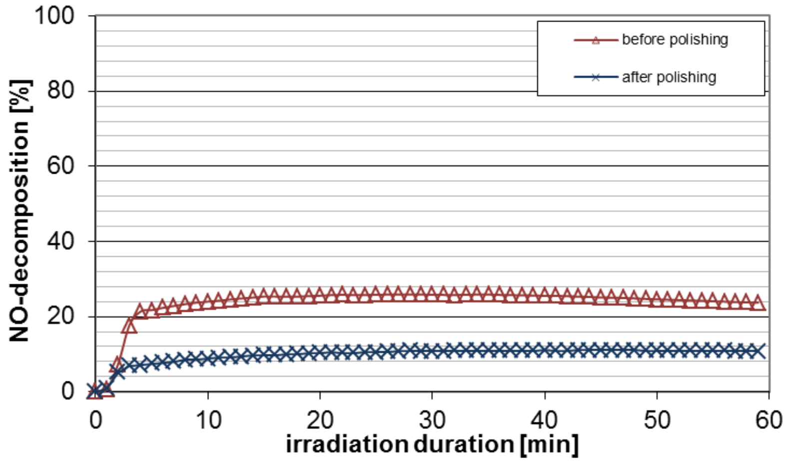

Figure 15: Reduction of nitric oxide before and after the polishing load to the samples on the test track

In addition to the NO decomposition rate, the pendulum test value, W/S value, and outflow time of the core samples were also measured after the polishing tests. As Table 3 shows, after 300 mins of APM polishing, both PTV-value and W/S-value are far beyond the minimum values according to the regulation set up by the German Road and Transportation Research Association [31, 32]. The outflow time was 1 s, which is far below the maximum guiding value of 30 s [31]. These post-polishing test results indicated that the spreading material has excellent durability of skid resistance and surface texture depth.

Table 3 Results of pendulum test, W/S test, and outflow test after 300 min polishing

Property	Test Results	Regulation Requirement
Pendulum Test Value	73	>65
W/S Value	0.61	>0.45
Outflow Time (s)	1	<30

7. Conclusions and future study

Within the scope of this study, a new method to build asphalt pavements with the function of NOx degradation was developed. In this method, TiO_2-containing spreading material was prepared by pulverizing custom-designed TiO_2-cement mortar, and then bonded to asphalt pavement surface by epoxy. The feasibility and performance of this method to degrade NOx under practical conditions were evaluated. It was found that durable NO-decomposition function and skid resistance of asphalt pavements can be achieved with the developed method and designed spreading material. In addition, field application indicated that the method allows the surface treatment of asphalt pavements to be completed within a few hours, enabling early traffic opening.

Further research is desired on the optimization of cement mortar grains in terms of their compressive strength, wearing resistance, and processability during construction. Furthermore, the durability of the treated asphalt pavement surface has to be further investigated, since the different thermal expansion properties of epoxy resin and asphalt could lead to cracking at the epoxy-asphalt interface when there are strong temperature fluctuations. Finally, life cycle cost analysis and environmental impact assessment in terms of practical application of the method should be conducted in future.

8. Acknowledgement

The work underlying this project was carried out under FE 09.0146/2010/HRB on behalf of the Federal Ministry of Transport and Digital Infrastructure in Germany, represented by the Federal Highway Research Institute.

9. References

[1] Stempihar, J. J., T. P. Manzouri, K. E. Kaloush, and M. C. Rodezno. Porous Asphalt Pavement Temperature Effects for Urban Heat Island Analysis. *Transportation Research Record: Journal of the Transportation Research Board*, No. 2293, Transportation Research Board of the National Academies, Washington, D.C., 2012, pp. 123-130.

[2] Losa, M., P. Leandri, and G. Licitra. Mixture Design Optimization of Low-Noise Pavements. *Transportation Research Record: Journal of the Transportation Research Board*, No. 2372, Transportation Research Board of the National Academies, Washington, D.C., 2013, pp. 25-33.

[3] Ballari, M. M., and H. J. H. Brouwers. Full Scale Demonstration of Air-purifying Pavement. *Journal of Hazardous Materials*, Vol. 254, 2013, pp. 406-414.

[4] Atkinson R. Atmospheric Chemistry of VOCs and NO_X. *Atmospheric Environment*, Vol. 34, No. 12, 2000, pp. 2063-2101.

[5] Chen, M., and Y. Liu. NO_X Removal from Vehicle Emissions by Functionality Surface of Asphalt Road. *Journal of Hazardous Materials*, Vol. 174, No. 1, 2010, pp. 375-379.

[6] Dylla, H., M. M. Hassan, L. N. Mohammad, T. Rupnow, and E. Wright. Evaluation of Environmental Effectiveness of Titanium Dioxide Photocatalyst Coating for Concrete

Pavement. *Transportation Research Record: Journal of the Transportation Research Board*, No. 2164, Transportation Research Board of the National Academies, Washington, D.C., 2010, pp. 46-51.

[7] Shen, S., M. Burton, B. Jobson, and L. Haselbach. Pervious Concrete with Titanium Dioxide as A Photocatalyst Compound For A Greener Urban Road Environment. *Construction and Building Materials*, Vol. 35, 2012, pp. 874-883.

[8] Hassan, M., H. Dylla, S. Asadi, L. N. Mohammad, and S. Cooper. Laboratory Evaluation of Environmental Performance of Photocatalytic Titanium Dioxide Warm-Mix Asphalt Pavements. *Journal of Materials in Civil Engineering*, Vol. 24, 2011, pp. 599-605.

[9] Hassan, M., L. N. Mohammad, S. Asadi, H. Dylla, and S. Cooper. Sustainable Photocatalytic Asphalt Pavements for Mitigation of Nitrogen Oxide and Sulfur Dioxide Vehicle Emissions. *Journal of Materials in Civil Engineering*, Vol. 25, No. 3, 2012, pp. 365-371.

[10] Leng, Z., and H. Yu. A Novel Method of Coating Titanium Dioxide onto Asphalt Pavements Based on Breath Figure Process for Air-purifying Purpose. *Journal of Materials in Civil Engineering*, 10.1061/(ASCE)MT.1943-5533.0001478, 04015188. 2015.

[11] Venturini, L., and M. Bacchi. Research, Design, and Development of a Photocatalytic Asphalt Pavement. *Proceedings of 2nd International Conference on Environmentally Friendly Roads: ENVIROAD*, October, 2009.

[12] Liu, W., S. Wang, J. Zhang, and J. Fan. Photocatalytic Degradation of Vehicle Exhausts on Asphalt Pavement by TiO2/Rubber Composite Structure. *Construction and Building Materials*, Vol. 81, 2015, pp. 224-232.

[13] Carneiro, J.O., S. Azevedo, V. Teixeira, F. Fernandes, E. Freitas, H. Silva, J. Oliveira. Development of Photocatalytic Asphalt Mixtures by the Deposition and Volumetric Incorporation of TiO_2 Nanoparticles, *Construction and Building Materials*, 38, 2013, pp. 594-601.

[14] Chen, M. and J.W. Chu. NOx Photocatalytic Degradation on Active Concrete Road Surface - from Experiment to Real-Scale Application. *Journal of Cleaner Production*, Vol. 19, Issue 11, 2011, pp. 1266-1272.

[15] Fujishima, A. Electrochemical Photolysis of Water at A Semiconductor Electrode. *Nature*, Vol. 238, 1978, pp. 37-38.

[16] Agrios, A.G., and P. Pichat. State of The Art and Perspectives on Materials and Applications of Photocatalysis over TiO_2. *Journal of Applied Electrochemistry*, Vol. 35, No.7, 2005, pp. 655-663.

[17] Zhao, J., and X. Yang. Photocatalytic Oxidation for Indoor Air Purification: A Literature Review. *Building and Environment*, Vol. 38, No. 5, 2003, pp. 645-654.

[18] Chen, J., and C. Poon. Photocatalytic Construction and Building Materials: From Fundamentals to Applications. *Building and Environment*, Vol. 44, No. 9, 2009, pp. 1899-1906.

[19] Dylla, H., M. M. Hassan, and L. J. Thibodeaux. Kinetic Study of Photocatalytic Degradation of Emitted Nitrogen Monoxide Using Titanium Dioxide Nanoparticles in

Concrete Pavements. *Transportation Research Record: Journal of the Transportation Research Board*, No. 2717, CD-ROM. Transportation Research Board of the National Academies, Washington, D.C., 2014.

[20] Wang, D., A. Schacht, X. Chen, P. Liu, M. Oeser, and B. Steinauer. Innovative Treatment to Winter Distresses Using a Prefabricated Rollable Pavement Based on a Textile-Reinforced Concrete. *Journal of Performance of Constructed Facilities*, 10.1061/(ASCE)CF.1943-5509.0000719, C4014008, 2014.

[21] ISO 22197-1. Fine Ceramics (Advanced Ceramics, Advanced Technical Ceramics) - Test Method for Air Purification Performance of Semiconducting Photocatalytic Materials - Part 1: Removal of Nitric Acid, 2008.

[22] Wang, D., A. Schacht, X. Chen, M. Oeser, and B. Steinauer. Machbarkeitsstudie für die Innovative Bauweise "Vorgefertigte und aufrollbare Straße". *Bautechnik*, 90(10), 2013, pp. 614-621.

[23] Wang, D., X. Chen, C. Yin, H. Stanjek, M. Oeser, and B. Steinauer. Influence of Freeze-Thaw on the Polishing Resistance of Coarse Aggregates on Road Surface. *Construction and Building Material*, 64, 2014, pp. 192-200.

[24] Wang, D., and X. Chen, C. Yin, M. Oeser, H. Stanjek, and B. Steinauer. Study of Micro-texture and Skid Resistance Change of Granite Slabs during the Polishing with the Aachen Polishing Machine. *Wear,* 318, 2014, pp. 1–11.

[25] EN 196-1 (2005). Methods of Testing Cement - Part 1: Determination of Strength, 2005.

[26] Bruse, M., and K. Droll. Betonbauteile mit Photokatalytisch Aktivierten Oberflächen-eine Chance zur Reduzierung des NO_x-Gehalts in Städten: Untersuchungsergebnisse und Modellierungsansätze, Proceedings of Kolloquium Luftqualität an Straßen 2011, Bergisch-Gladbach, March 2011, pp. 236-258.

[27] De Buhr, S.: Untersuchungen zur Eignung von TiO_2 zur Photokatalystischen Reinigung von Kraftfahrzeugabgasen, PhD Thesis, Universität Hannover, 2005.

[28] Wang, D., X. Chen, C. Yin, M. Oeser, and B. Steinauer. Influence of Different Polishing Conditions on the Skid Resistance Development of Asphalt Surface. *Wear*, 308, 2013, pp. 71-78.

[29] The Technical Delivery Terms for Aggregates in Road Construction (TL Gestein-StB 04), Edition 2004/Version 2007.

[30] EN 1097-2, Tests for Mechanical and Physical Properties of Aggregates – Part 2: Methods for the Determination of Resistance to Fragmentation, 2010.

[31] The Guideline for the Assessment of Road Skid Resistance in Wet Condition, German Road and Transportation Research Association, 2012.

[32] Huschek, S.: Die Griffigkeitsprognose mit der Verkehrssimulation nach Wehner/Schulze, Bitumen, S. 14-18, 01/2002.